

VIBRATION BEHAVIOUR OF THE MTC EXPERIMENTAL SUBWAY WHEEL

L. Strasberg, J. Tiessinga and K. Kono

Research and Development Division
Ontario Ministry of Transportation and Communications

ABSTRACT

The natural frequencies, mode shapes, and mechanical impedances of a resilient type subway wheel are presented. An impact method which uses Fourier techniques to analyse the vibrations of the wheel is described. Several natural frequencies and mode shapes not previously reported are presented.

INTRODUCTION

Rail transportation operating authorities consider railway noise a serious enough problem to commit large expenditures of capital and technology in an attempt to reduce it. The United States Department of Transportation, for example, has recently published a report which assesses the noise problems in several railed urban systems in the United States [1]. The South-East Pennsylvania Transit Authority (SEPTA) is testing ring damped wheels for the American Public Transit Association (APTA) [2]. In Canada, the Ontario Ministry of Transportation and Communications (MTC) has built several experimental streetcar and subway wheels with the aim of obtaining a better understanding of the wheel/rail noise problem [3].

It is believed that wheel/rail noise contributes a significant portion of the total noise emitted from electrically powered trains [4]. Because the noise associated with the wheel and rail comes about as a result of these components vibrating within the audible frequency range, it follows that reductions in these vibrations should abate the sound levels - provided the surface areas of the vibrating parts and their sound radiation efficiencies do not change in an adverse direction. In order to better understand the vibrating systems involved, the MTC is currently investigating the dynamic behaviour of several railway wheels.

This paper presents the results obtained when one MTC experimental wheel, the subway wheel shown in Fig. 1, was excited at frequencies within the audible frequency range. An impact technique was used. The dynamic parameters presented include the natural frequencies of the wheel, their associated mode shapes and some of the mechanical driving-point impedances and transfer impedances of the wheel.

EXPERIMENTAL PROCEDURE

The wheel was supported on rubber pads which were themselves mounted on a low frequency wooden platform of the type shown in Ref. 3. This support arrangement ensured that the wheel was in the free-free state. The wheel was struck by a specially made hammer to which a load cell was attached. An accelerometer was suitably positioned on the wheel. The signals from the load cell and from the accelerometer were routed to a dual-channel Fast Fourier Transform Analyser for processing. This instrument will rapidly break down both input signals into their Fourier components. In addition the machine is capable of performing several mathematical functions on these signals. The functions of interest for this paper include integration and differentiation. In addition, the instrument is capable of comparing signals (viz., by division) in both the time and frequency domains.

An ideal impulse may be considered as a dirac delta function, theoretically an infinite force acting for zero time. Fourier analysis on this signal will transform it into a continuous force signal throughout the entire frequency range. The signal obtained from the load cell attached to the hammer represents the impulse used to excite the MTC wheel. A typical signal is illustrated in Figs. 2 and 3 as channel B. In Fig. 2, it is seen that the impulse actually used had finite values for both the applied force and the time over which it acts. When Fourier analysis is used to transform this time varying signal into the frequency domain (Fig. 3), it is clear that the frequency content of the impact is also limited. This is not considered a serious limitation to the results because the upper frequency limit (15 kHz) is quite near to that of the human ear.

The vibration of the wheel resulting from the impact, is presented as channel A in Figs. 2 and 3. The first figure shows the vibration in the time domain, the second in the frequency domain. Because channel A in Fig. 3, shows the magnitude of the response at any given frequency, the peaks in the data represent those frequencies at which the wheel exhibits its maximum responses, ie. its natural frequencies.

The response of the wheel that results from excitation at various points is compared by using a quantity known as mechanical impedance. The mechanical driving-point impedance of the system is defined as the ratio of the force acting at a given point in a system to the resulting velocity at that point. It is a complex quantity having magnitude and phase, and is a function of the frequency of excitation. When the velocity is measured at a point other than the point of excitation, the term "transfer impedance" will be used. The input force for each investigation was measured via the load cell in the hammer (channel B) and the resulting velocity was obtained by integrating the output signal of the accelerometer on the wheel (channel A). The impedance was obtained as the ratio of channels B to A. Figure 4 shows a typical set of results obtained in this manner. Note that the natural frequencies of the wheel show up as steep "valleys" in this plot, ie. those frequencies at which a minimum of force gives a maximum amount of response. The results are presented in a slightly different form in Fig. 5 where the real and imaginary components are illustrated. The coherence between the signals is shown in Fig. 6.

RESULTS

Some of the results of these investigations are presented in Figs. 7 to 26.

The lateral point impedances of the MTC subway wheel are shown in Fig. 7. They were obtained by placing the accelerometer laterally on the front face of the rim, and striking the wheel laterally at a point as close as possible to the accelerometer. The natural frequencies obtained were essentially the same as those previously reported [3].

The mode shapes (Fig. 7) associated with the natural frequencies, were obtained with the aid of transfer impedances. The wheel was struck laterally on the rim at several different circumferential positions while the accelerometer remained at a reference location. Transfer impedances were thus obtained for the spatial locations shown in Figs. 8 to 14. By examining the impedances at the frequencies of interest, the resistance to motion of several points on the wheel were determined. Recalling that vibratory motion is assumed to be simple harmonic and by using the inverse of impedance, ie. mobility, the lateral motions of all points on the rim of the wheel were determined at each frequency of interest. Figures 15 and 16 show the plots obtained when the data associated with two of the natural frequencies were used in this manner. The remaining mode shapes were found by similar methods.

The modes of vibration shown in Fig. 7 are due to the out-of-plane bending of the rim. Similar modes have been found by Stappenbeck [5] and by Strasberg [6]. These are the modes usually associated with squeal noise in lightly damped wheels [6]. In the subway wheel under investigation, rubber blocks were used to improve the damping ratios and hence lead to lower squeal noise levels. The damping ratios associated with these modes of vibration are presented elsewhere [3,6].

The radial impedances of the wheel tested are shown in Figs. 17 to 24. They were obtained in a manner similar to that described above, except that the tread of the wheel (ie., its running surface) was used for both mounting the accelerometer and as the location where the wheel was struck.

The mode shapes shown in Fig. 17 are associated with in-plane bending of the rim of the wheel. They, too, were obtained in a manner similar to that described above. As far as can be determined by a search of the relevant literature, many of these in-plane bending modes have not been previously reported. This may be a consequence of the method normally used to determine the mode shapes of a wheel, viz. to spread particles on the web of a wheel which is supported in the horizontal plane and then to shake the wheel at the frequency of interest. It is expected that a standard wheel would exhibit similar in-plane bending modes. However, for any given mode, the stiffer rim of the standard wheel should lead to a higher natural frequency than that associated with the thinner rim of the resilient wheel.

CONCLUSIONS

The radial and lateral impedances of an MTC subway type resilient wheel have been obtained. These mechanical impedances when used in conjunction with other relevant parameters, eg. surface areas and sound radiation efficiencies, may be used to predict the noise from this wheel.

Several vibrating modes, not previously reported, have been identified for a resilient railway wheel. These are shown to be associated with the in-plane bending of the rim of the wheel.

REFERENCES

1. Chisholm, G., et al, "National Assessment of Urban Rail Noise", Report No. UMTA-MA-06-0099-79-2, U.S. Department of Transportation, Urban Mass Transportation Administration, Office of Technology Development and Deployment, Office of Rail and Construction Technology, Washington, D.C. 20590, March 1979.
2. SEPTA Noise and Vibration Study, Contract No. DOT-TSC-1053 , U.S. Department of Transportation, Transportation Systems Center, Kendall Square, Cambridge, MA 02142, 1978.
3. Strasberg, L., Perfect, N., Elliot, G.L., "Properties of Railway Wheels", Acoustics and Noise Control in Canada 6, 2, April 1978. Published by the Canadian Acoustical Association.
4. Remington, P.J. et al, "Wheel/Rail Noise and Vibration", Report No. UMTA-MA-06-0025-75-10, U.S. Department of Transportation, Urban Mass Transportation Administration, Office of Research and Development , Rail Technology Division, Washington, D.C. 20590, 1975
5. Stappenbeck, H., "Das Kurvengeräusch der Strassenbahn" Verein Deutscher Ingenieure, 1954, 96 (b), 171-176.
6. Strasberg, L., Perfect, N., Elliott, G.L., "Some Static and Dynamic Properties of Railway Wheels", Publication 78-WA/RT-4, The American Society of Mechanical Engineers, United Engineering Center, 345 East 47th Street, New York, N.Y. 10017.

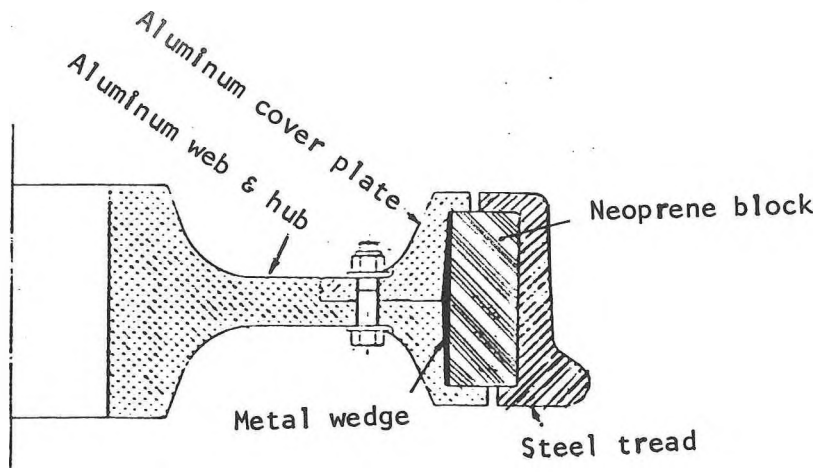


FIGURE 1: MTC Experimental Subway Wheel

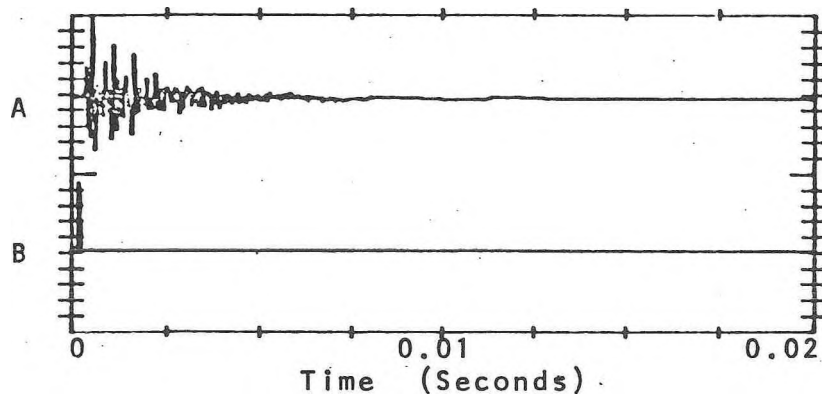


FIGURE 2: Time Response of Wheel (A) due to Hammer Blow (B)

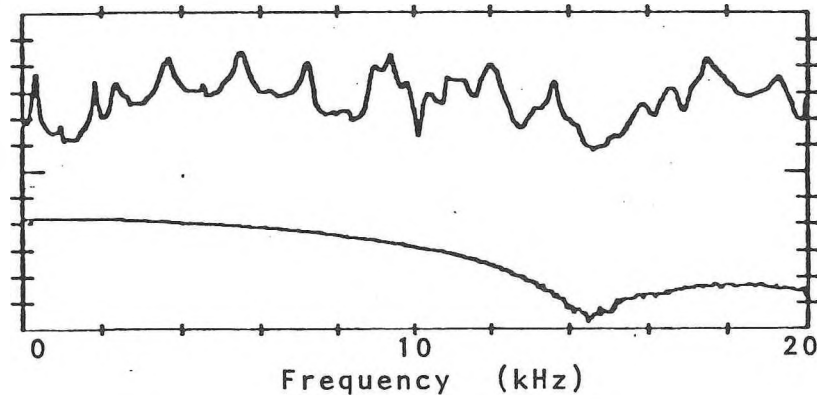


FIGURE 3: Frequency Response of Wheel (A) due to Hammer Blow (B)

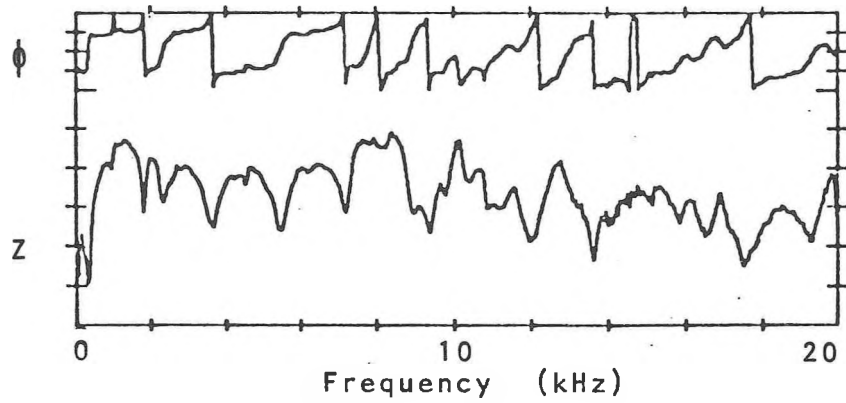


FIGURE 4: Impedance of Wheel (Typical Results)

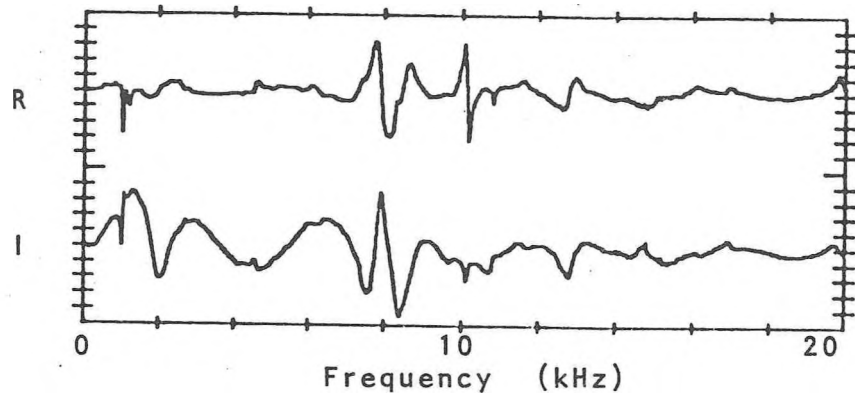


FIGURE 5: Impedance of Wheel (Typical Results)

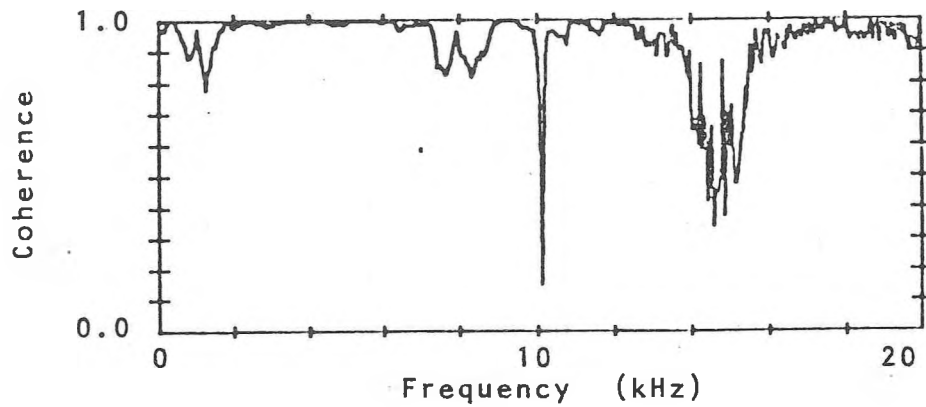


FIGURE 6: Coherences (Typical Results)

Note: Number of Nodal Circles not determined for these modes.

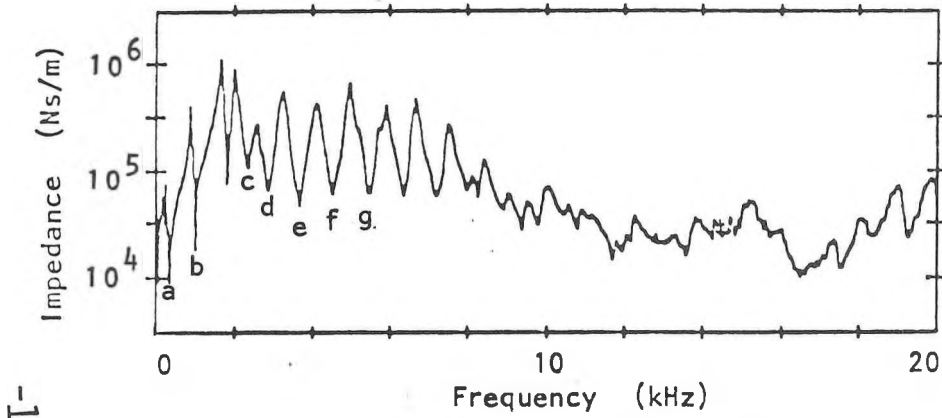
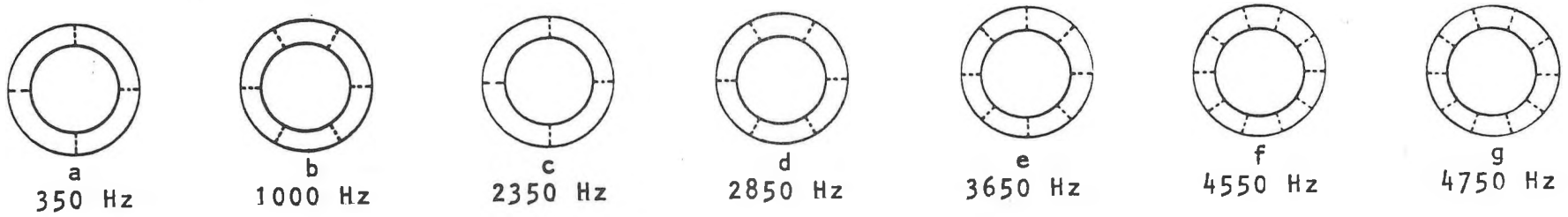


FIGURE 7: Lateral Point Impedance taken at 0°

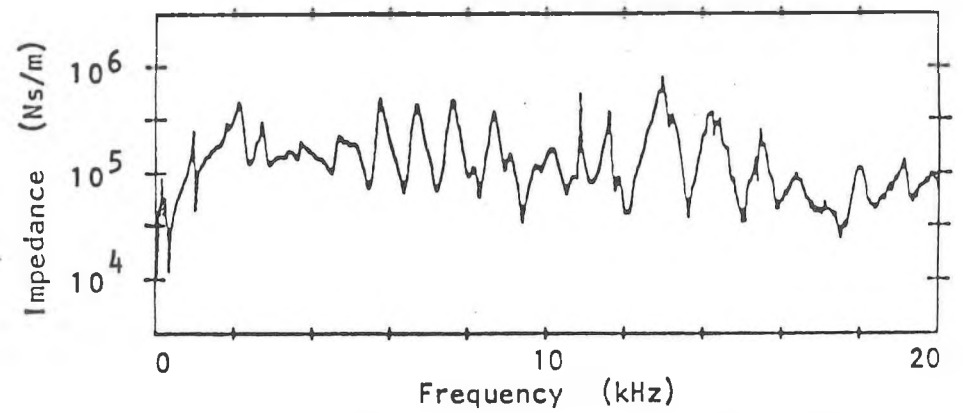


FIGURE 8: Lateral Transfer Impedance taken at $22\frac{1}{2}^\circ$

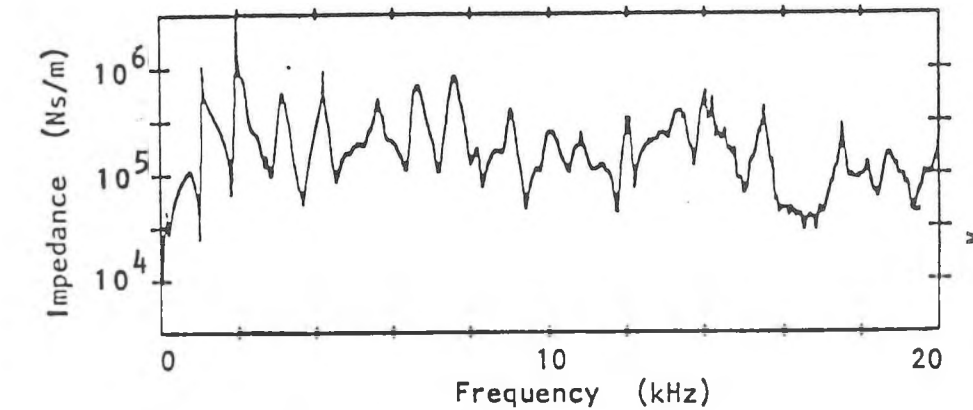


FIGURE 9: Lateral Transfer Impedance taken at 45°

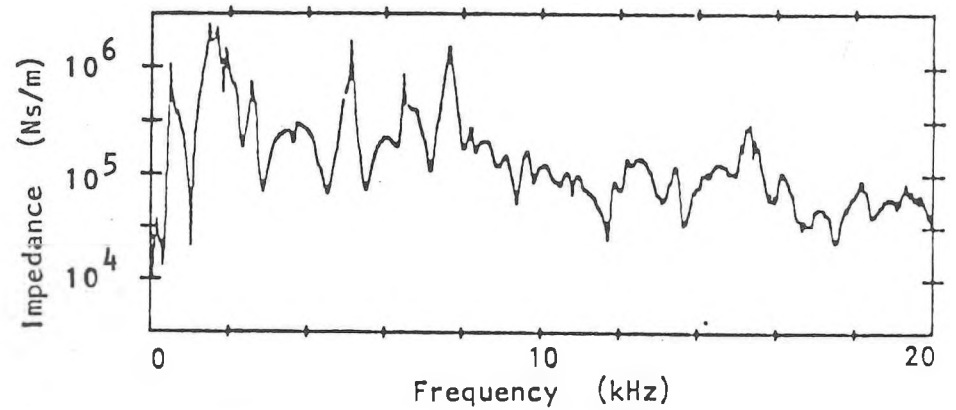


FIGURE 10: Lateral Transfer Impedance taken at $67\frac{1}{2}^\circ$

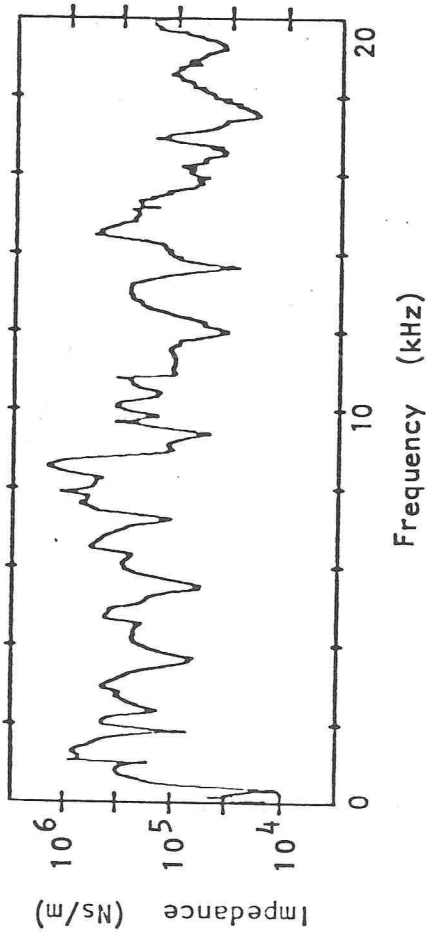


FIGURE 11: Lateral Transfer Impedance taken at 90°

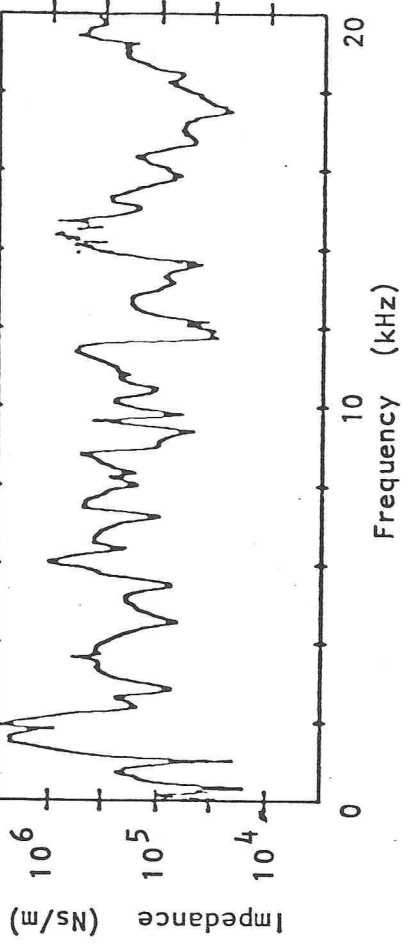


FIGURE 12: Lateral Transfer Impedance taken at $112\frac{1}{2}^\circ$

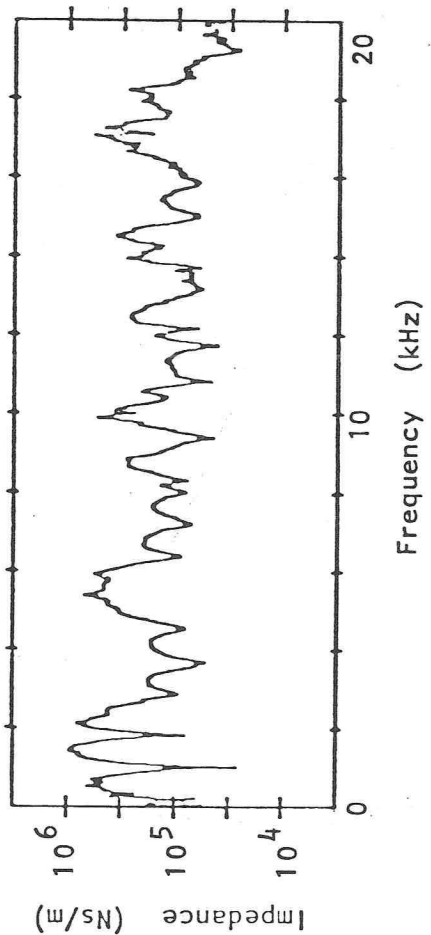


FIGURE 13: Lateral Transfer Impedance taken at 135°

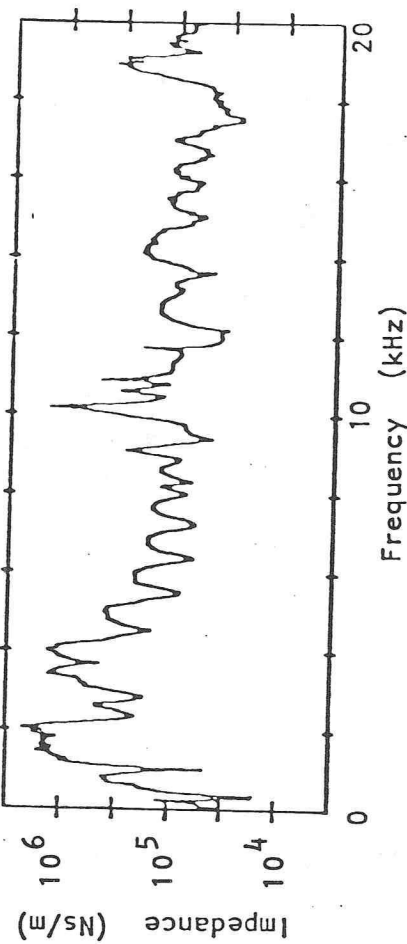


FIGURE 14: Lateral Transfer Impedance taken at $157\frac{1}{2}^\circ$

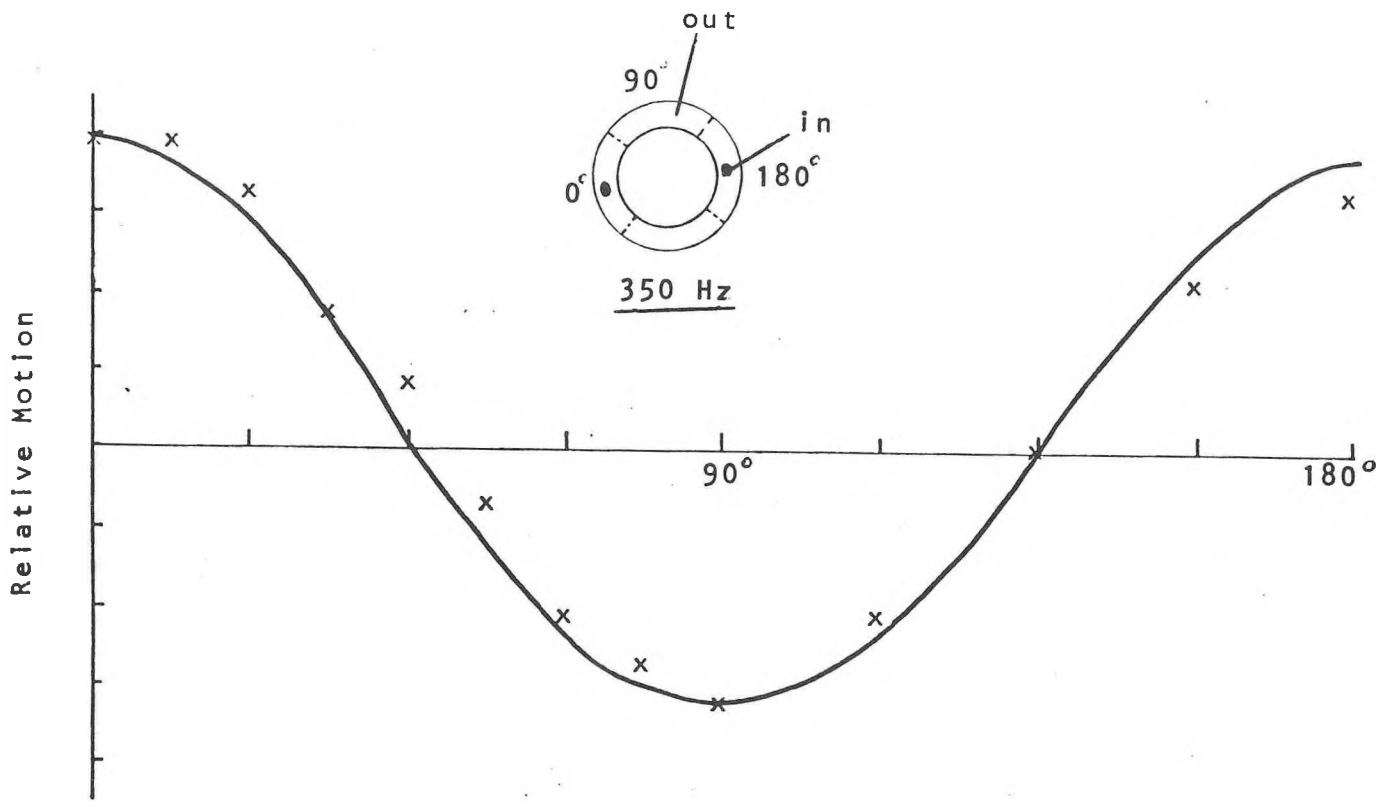


FIGURE 15: Relative Motion of Rim in Lateral Direction

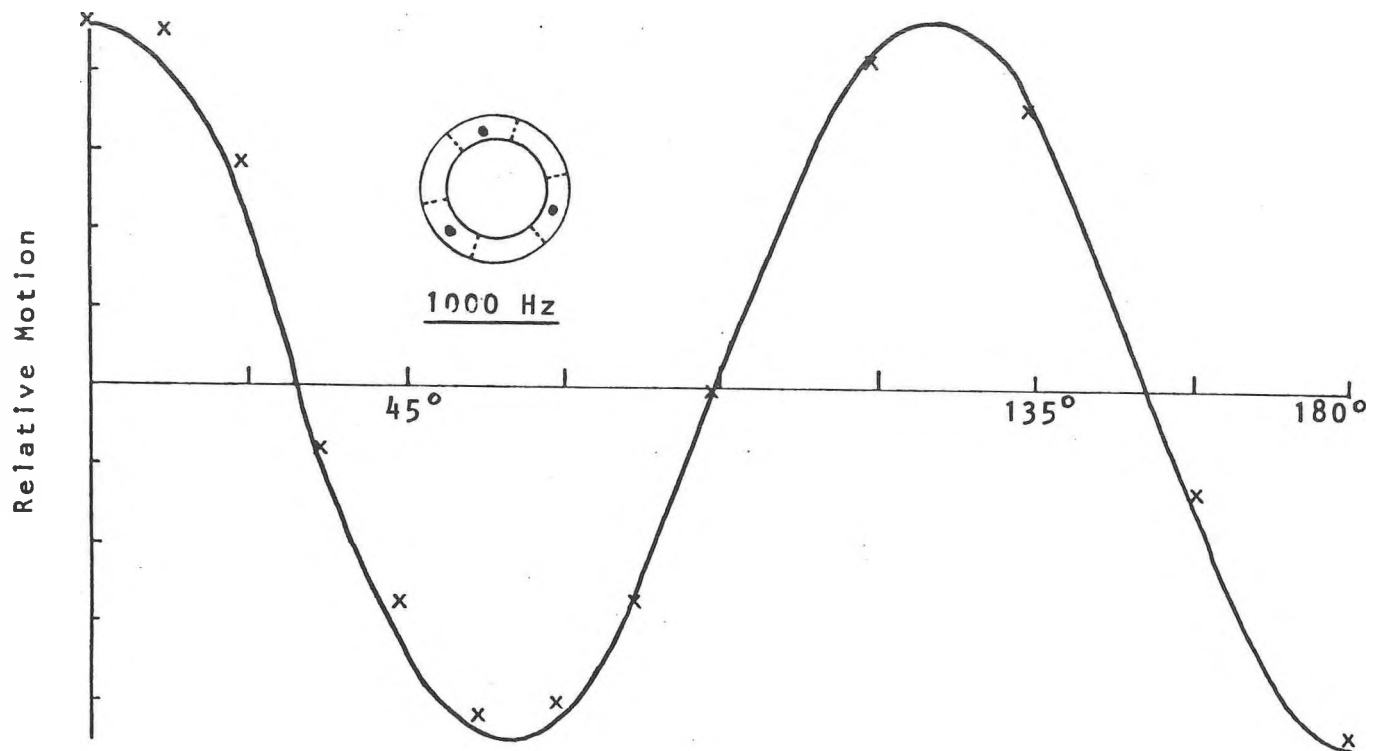


FIGURE 16: Relative Motion of Rim in Lateral Direction

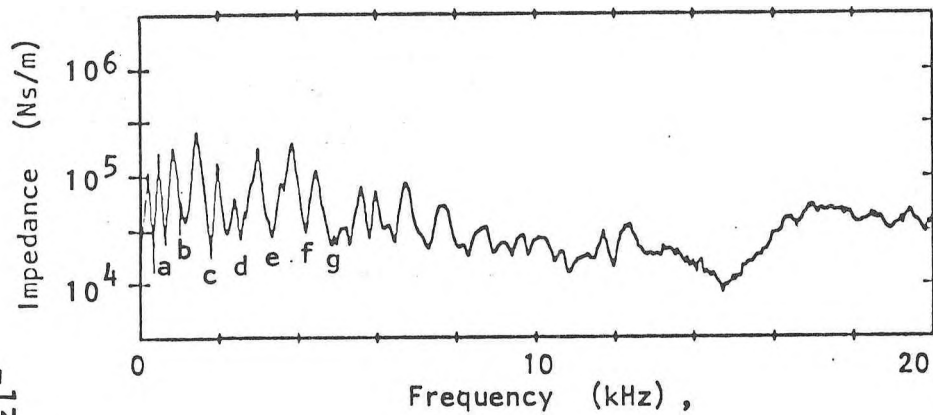
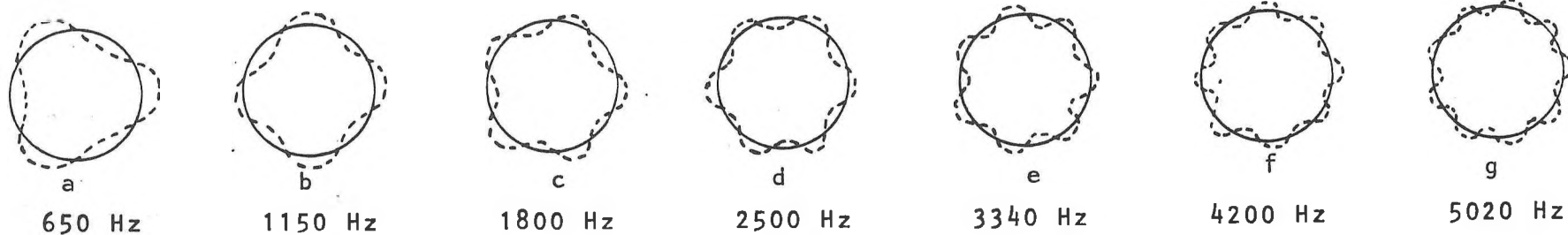


FIGURE 17: Radial Point Impedance taken at 0°

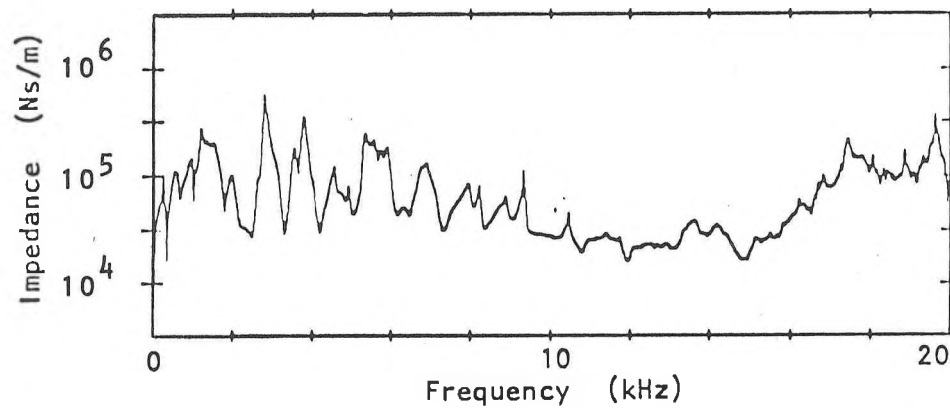


FIGURE 18: Radial Transfer Impedance taken at $22\frac{1}{2}^\circ$

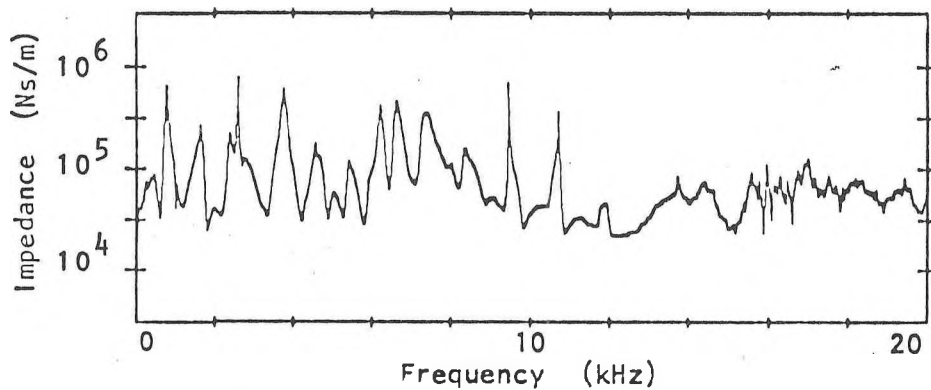


FIGURE 19: Radial Transfer Impedance taken at 45°

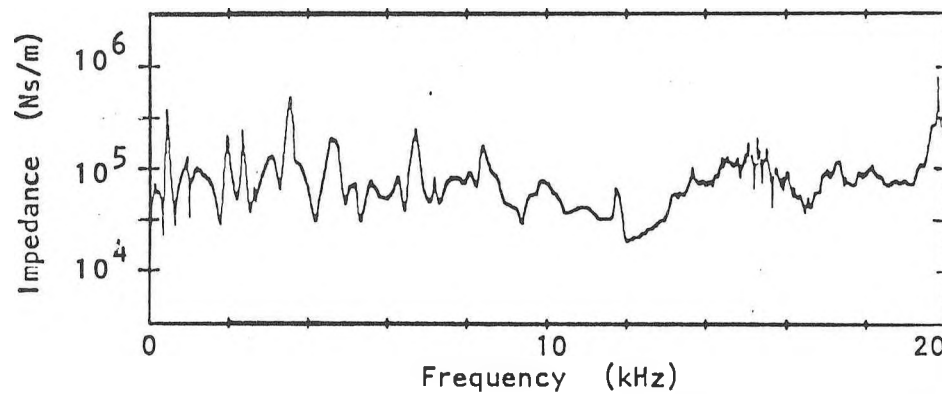


FIGURE 20: Radial Transfer Impedance taken at $67\frac{1}{2}^\circ$

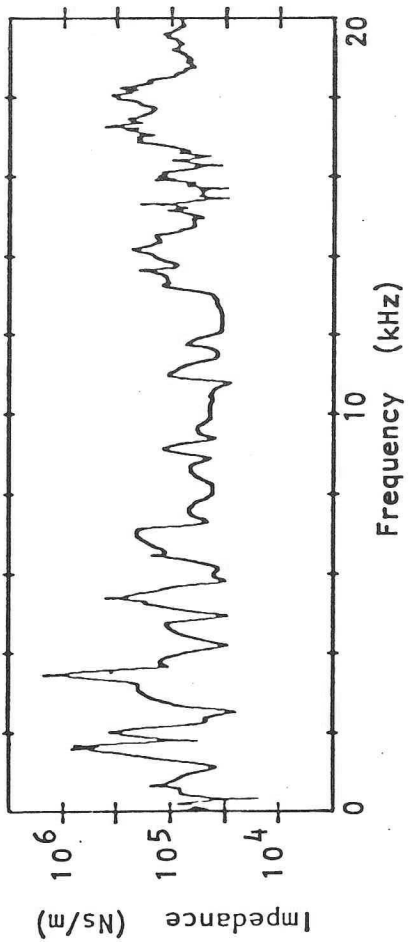


FIGURE 21: Radial Transfer Impedance taken at 90°

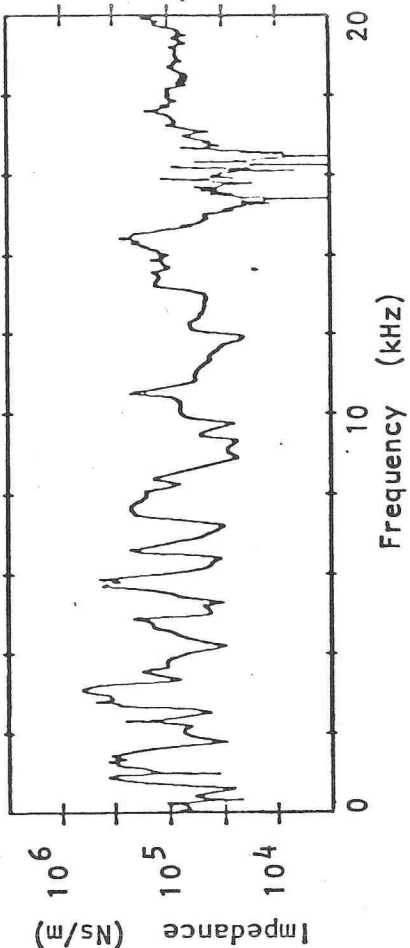


FIGURE 22: Radial Transfer Impedance taken at $112\frac{1}{2}^\circ$

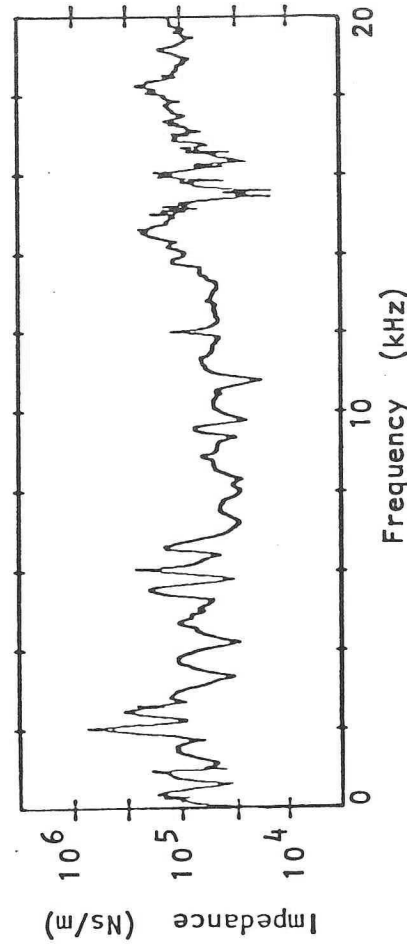


FIGURE 23: Radial Transfer Impedance taken at 135°

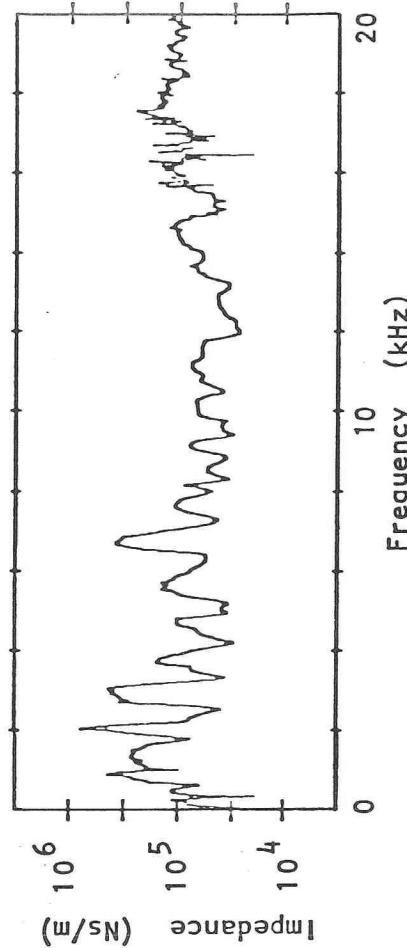


FIGURE 24: Radial Transfer Impedance taken at $157\frac{1}{2}^\circ$

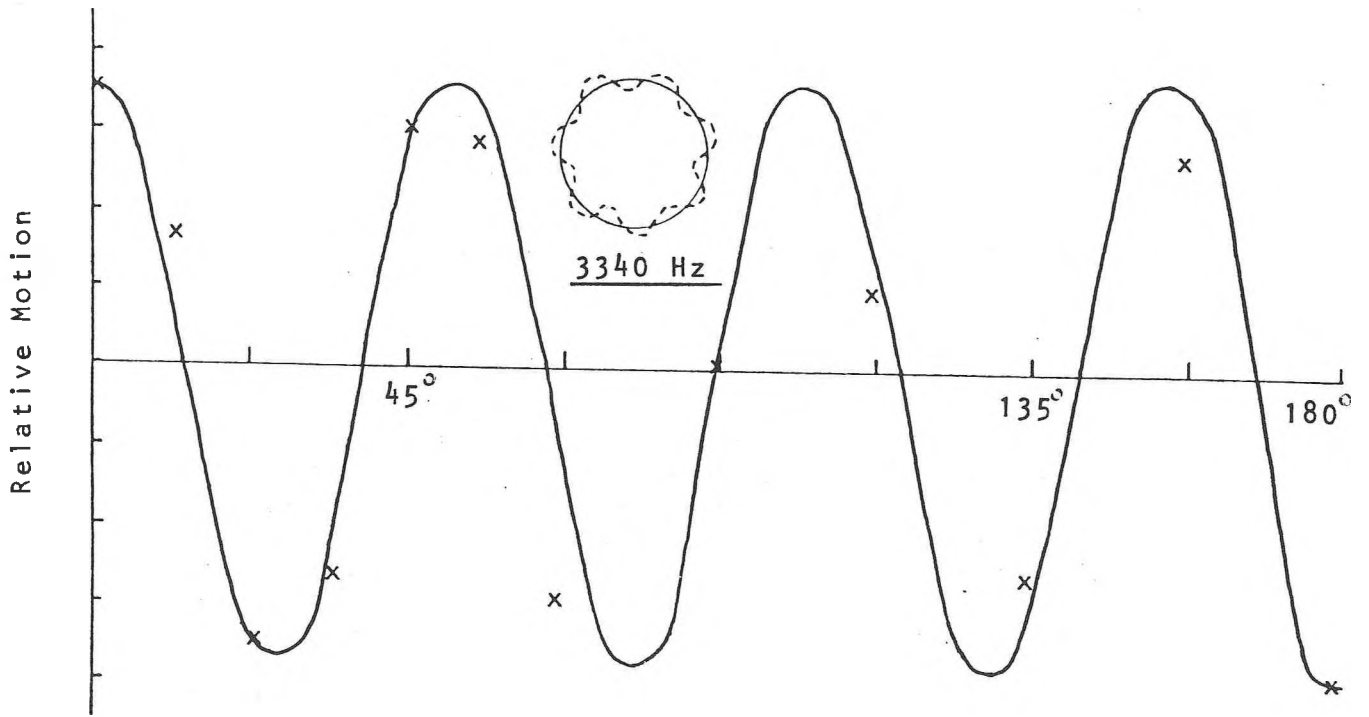


FIGURE 25: Relative Motion of Rim in Radial Direction

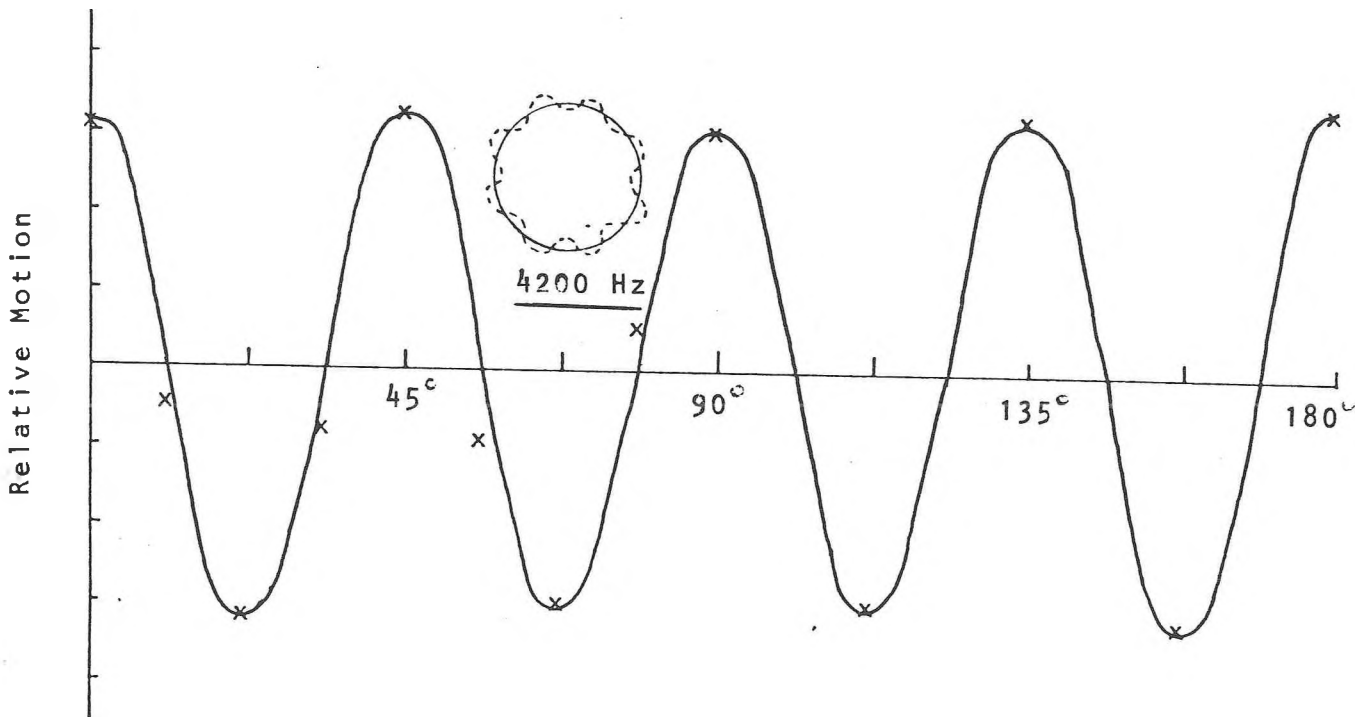


FIGURE 26: Relative Motion of Rim in Radial Direction